VECTOR SEGMENTATION OF VOLUMETRIC IMAGE DATA
Tetrahedral Meshing Constrained by Image Edges

Michal Španěl, Přemysl Kršek, Miroslav Švub and Vít Štancl

Department of Computer Graphics and Multimedia
Faculty of Information Technology, Brno University of Technology, Czech Republic

Keywords: CT/MR data, Medical image segmentation, Surface reconstruction, Delaunay triangulation, Variational tetrahedral meshing, Isotropic meshing, Graph-cut segmentation.

Abstract: In this paper, a vector segmentation algorithm of volumetric data based on the 3D Delaunay triangulation is presented. A modified variational meshing method is used to adapt tetrahedral mesh to the underlying CT/MRI volumetric data. Moreover, to classify tetrahedra in the mesh into regions whose characteristics are similar, a clustering scheme viewing the mesh as undirected graph with edges weighted according to similarity of tetrahedra is discussed.

1 INTRODUCTION

Traditional raster-based segmentation methods produce data which are not suitable for geometrical 3D modeling. Most often, an algorithm such as Marching Cubes (Lorensen and Cline, 1987) is applied to reconstruct surfaces from the raster data. Therewith, further decimation and smoothing of the model are required.
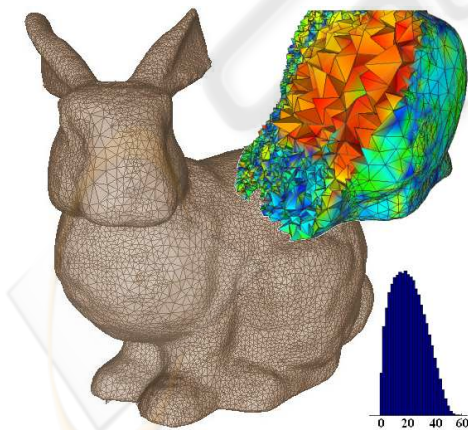

Figure 1: Result of the proposed tetrahedral meshing method, and histogram of the minimal dihedral angles in the final mesh. The bunny was printed using rapid prototyping machine (3D printer) and scanned on a CT machine. Afterwards, the volumetric data was processed.

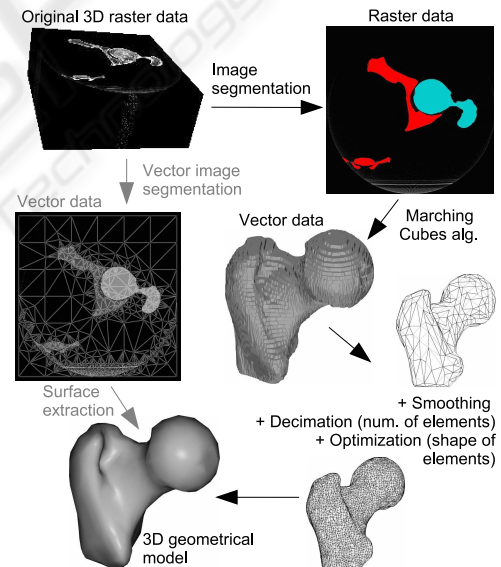Principal task of an image segmentation is the im-

Figure 2: Comparison of the traditional raster-based segmentation (black labeling) and the presented vector segmentation method (gray).

age partitioning into a set of non-overlapping regions so that variation of some property within each region follows a simple model. It has been shown that 2D *Delaunay triangulation* can be used to effectively partition the image (Gevers, 2002), while the mesh is adapted to the image structure by combining region and edge information.

In this paper, recent advances in a vector segmen-

tation technique based on a *3D Delaunay Triangulation* are presented. This work follows principles previously described in (Spanel et al., 2007). Tetrahedral mesh is used to partition volumetric image data into regions (see Figure 2). Process of the mesh construction respects significant image edges, so surfaces of image regions are well described and can be easily derived.

2 TETRAHEDRAL MESHING

A mesh generation (George and Borouchaki, 1998) aims at tessellation of a bounded 3D domain Ω with tetrahedra. Algorithms for 3D mesh generation have been intensively studied over the last years. Basically, three main families of algorithms have been described: Octree methods, Advancing front methods, and Delaunay-based methods (Owen, 1998).

2.1 Delaunay Triangulation (DT)

Every tetrahedron of the DT satisfies the *Delaunay criterion*. This criterion means that circumsphere associated with the tetrahedron does not contain any other vertices. This criterion is a characterization of the Delaunay triangulation. The Delaunay triangulation generates regularly shaped tetrahedra and is very attractive from a robustness point of view due to simplicity of the Delaunay criterion.

Constrained Delaunay triangulation (CDT) is a triangulation where constraints given as set of edges and faces in 3D remain as entities of the resulting mesh. There are two classes of methods depending on how the constraints must be satisfied. The first kind acts by local modifications to enforce the given constraints, while the other kind tends to modify the constraints and creates an admissible set of constraints.

A *Constraint partitioning method* is a simple representative of the second class. Every tetrahedron intersected by a constrained edge/face is divided ensuring that the created sub-edges are in the resulting triangulation. Advantage of the constraint partitioning method is that it can be easily extended to 3D.

Many *Delaunay refinement* methods (Shewchuk, 2002) exist that improve tetrahedra locally by inserting new nodes to maintain the Delaunay criterion.

2.2 Isotropic Meshing

Many applications have specific requirements on the size and shape of elements in the mesh. The aim of the isotropic meshing is to locate vertices so that the resulting mesh consists of almost equilateral tetrahedra.

In addition, the element size is close to a predefined size constraint.

One of the existing methods to create vertices in accordance with the size specifications, *creation of points along the edges*, is discussed in (George and Borouchaki, 1998). The idea is to create new points along existing edges in the triangulation and obtain nearly equilateral tetrahedra having edges of length *h*. In (Spanel et al., 2007), this method has been modified for isotropic meshing of volumetric image data.

2.3 Variational Tetrahedral Meshing

Many approaches based on energy minimization (Du and Wang, 2003) have been proposed as a powerful tool in meshing. In this paper, a vector segmentation technique, built upon a *Variational Tetrahedral Meshing* approach (Alliez et al., 2005), is presented. A simple minimization procedure alternates two steps:

- Delaunay triangulation optimizing connectivity,
- local vertex relocation,

to consistently and efficiently minimize a global energy over the domain. It results in a robust meshing technique that generates high quality meshes in terms of radius ratios as well as angles.

To extend the approach to allow isotropic meshing, the sizing field H is introduced A *mass density* in space can be defined and used in computation of the optimal vertex position. This density should agree with the sizing field. Alliez uses a one-point approximation of the sizing field in a tetrahedron. In geometric terms, an optimal position of the interior vertex X_i in its 1-ring can be expressed as:

$$X_i^* = \frac{1}{\sum_{T_k \in \Omega_i} \frac{|T_k|}{h^3(G_k)}} \sum_{T_j \in \Omega_i} \frac{|T_j|}{h^3(G_j)} c_j. \qquad (1)$$

where G_k is the centroid of tetrahedron T_k.

In (Alliez et al., 2005), a default sizing field is proposed, robust for a large spectrum of mesh types. Definition of the sizing field is build on the notion of *local feature size* that corresponds to the combination of domain *boundary curvature* and *thickness* as well.

The local feature size $lfs(P)$ at a point P of domain boundary is defined as the distance $d(P, S(\Omega))$ to a *medial axis* $S(\Omega)$. The medial axis, or skeleton, is the locus of all centers of maximal balls inscribed in the boundary. Given the local feature size on the boundary, we need a controllable way to extrapolate this function to the interior. The function

$$h_P = \min_{S \in \delta\Omega}[Kd(P) + lfs(S)] \qquad (2)$$

satisfies this criterion. The parameter *K* controls gradation of the resulting field.

3 DELAUNAY-BASED VECTOR SEGMENTATION

Based on the introduced principles, the vector segmentation was originally proposed as follows:

1. *3D edge and corner detection* - Candidate vertices lying on regions boundaries, meaningful edges and corners are located.

2. *Initial Delaunay triangulation* - Tetrahedral mesh is constructed from the sampled set of candidate vertices by the common *Incremental Method* (George and Borouchaki, 1998).

3. *Iterative adaptation* - The triangulation is adapted to the underlying image structure.

4. *Mesh segmentation* - Classification of tetrahedra into image regions.

This paper introduces several changes in the original segmentation. The mesh of the DT is adapted to the image structure by means of isotropic edge splitting and variational meshing. The image is classified into regions using a graph-based clustering algorithm.

3.1 3D Edge and Corner Detection

The triangulation starts with a set of candidate vertices distributed over the entire image. In all our experiments, the well known *Canny edge detector* extended to the 3D space has been used.

In order to respect significant features in the volumetric data during the meshing, we have modified the *Susan corner detector* (Smith and Brady, 1996) extending its functionality into 3D space. The Susan (*Smallest Univalue Segment Assimilating Nucleus*) detector was originally developed to locate feature points in 2D images.

Analogous to *Smith and Brady*, the modified 3D SUSAN places a spherical mask R over the voxel to be tested (the nucleus). The voxel in this mask is represented by $v \in R$. The nucleus is at v_0. Every voxel is compared to the nucleus using a distance function c_v. Final response of the SUSAN detector is proportional to an area $n(R)$ of the SUSAN given by:

$$n(R) = \frac{1}{N} \sum_{v_i \in R} c_{v_i}. \tag{3}$$

In the equation (3), N is the number of voxels within a spherical mask R used as a normalization factor. If c_v is the rectangular function, then the previously defined area represents the number of voxels in the mask having brightness similar to the nucleus.
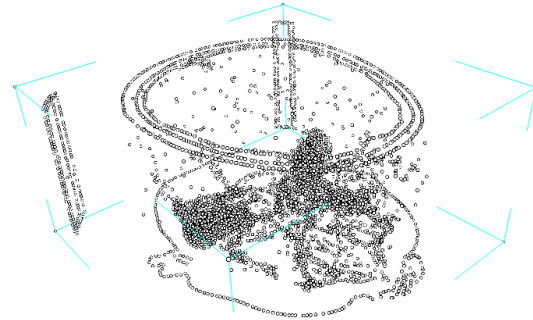

Figure 3: Sampled initial set of vertices found by the edge and corner detection.

3.2 Iterative Adaptation

Fundamental part of the proposed segmentation method is adaptation of the mesh to cover the underlying image structure. Following two main steps are repeated several times:

1. *Isotropic edge splitting* - creation of points along existing edges, introduces new points to the mesh.

2. *Variational meshing* - optimization of the tessellation grid by means of vertex moving.

Isotropic Edge Splitting. In this phase, the isotropic meshing algorithm *creating new points along existing edges* and another well known technique of tetrahedral mesh optimization, *splitting of maximal/longest edge*, are combined together. The splitting phase is similar to the one described in (Spanel et al., 2007). The only difference is definition of the sizing field, so called *control space*.

The control space prescribes length of edges in the mesh. In our case, control space enforces creation of larger tetrahedra inside image regions and smaller ones along region boundaries (image edges). Apparently, definition of the sizing field strongly affects quality of the final mesh.

In this sense, one can define the control space $H(\Omega)$ in the same way as the sizing field given by the equation (2). This definition is robust and produces high quality meshes. Instead of the conventional domain boundary, we define the control space to respect found image edges. Thus, we generate the control space differently:

1. Estimate *distance transform* from all detected image edges first.

2. Find local maxima of the distance transform in order to identify medial axis.

3. Evaluate local feature size $lfs(P)$ on image edges using inverse distance transform propagating value from the medial axis.

4. Generate control space distributing $lfs(P)$ from edges using the formula (2).

This sizing field is relative. It describes the inhomogeneity of required edge length. The real edge length is proportional to this relative value, and depending on the prescribed number of vertices.

Variational Meshing. The variational meshing phase, alternating connectivity and geometry optimization, is an important part of the algorithm. The energy is minimized by moving each *interior* vertex to its optimal position. Further, the energy is minimized by computing the 3D Delaunay triangulating of these new sites.

Analogous to (Alliez et al., 2005), the boundary vertices are treated differently. In order to identify the current boundary vertices, each voxel V_i lying on an image edge is examined. Its nearest vertex S_j in the mesh is located, and the distance $d(V_i, S_j)$ as well as the coordinates of V_i (multiplied by the distance d) are accumulated at that vertex. To deal with corner points, the distance d is weighted according to the point type. Corner points have the weight significantly greater than edge points, thus the closest vertex is attracted directly in place of the image corner.
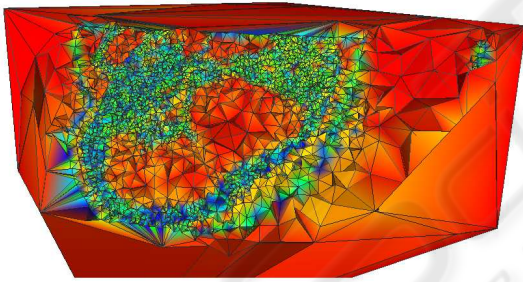

Figure 4: Result of the adaptation of the mesh ($K = 0.8$).

Afterwards, all vertices with a non-zero distance sum are the desired boundary vertices. These vertices are moved to the average value they each have accumulated during the pass over all edge voxels.

3.3 Mesh Segmentation

Every tetrahedron t_i of the mesh is characterized by its feature vector. Individual features detail image structure of the tetrahedron and its close neighbourhood. In fact, the first two components are mean pixel value and intensity variance of voxels inside the tetrahedron, other features may cover image texture.

Topology of the tetrahedral mesh is suitable for graph-based segmentation techniques. Instead of pixels and the traditional 4– and 8– pixel connectedness,

tetrahedra and graph adjacency are incorporated.

Graph-based Segmentation. Viewing the mesh as undirected graph, with edges weighted according to similarity of feature vectors, allows one to use graph algorithms (graph cuts, path algorithms, etc.) for the segmentation.

In our experiments, we have used the *Min-Cut/Max-Flow* algorithm proposed in (Boykov and Kolmogorov, 2004) to cut a graph whose edges are evaluated according to the similarity of two adjacent tetrahedra.

4 RESULTS AND DISCUSSION

The proposed segmentation algorithm was tested on a real CT imaging data (about $120 - 150$ slices, resolution 512x512 pixels per slice). The whole segmentation process, including iterative mesh adaptation and final classification, takes approximately $15 - 25$ minutes on standard PC with Intel DualCore 2.54GHz processor depending on concrete number of slices, and parameters of the meshing algorithm.

Results of the segmentation shown in Figure 5 outperforms the original method (Spanel et al., 2007). Especially, the overall mesh quality in the sense of shape of tetrahedra has been improved. In the Figure 5, histograms show distribution of the minimal dihedral angles within regions of the tetrahedral mesh.

The graph-based mesh segmentation algorithm designed for the unsupervised clustering of feature vectors performs almost same, sometimes slightly better, then the original method based on *Fuzzy C-means* and *GMM+EM* clustering techniques. Further improvement of the classification phase must incorporate more sophisticated image features modeling 3D texture and spatial image properties.

An inconvenience of the described meshing technique is that slivers appear in the mesh, especially close to the image edges. Regarding recent research in this area, methods like the modified *sliver exudation* (Cheng et al., 1999), or *sliver perturbation* must be incorporated in the meshing process in the future.

5 CONCLUSIONS

In this paper, the vector segmentation algorithm based on isotropic Delaunay triangulation proposed in (Spanel et al., 2007) is extended. To improve quality of the tetrahedral mesh, the variational meshing is utilized. Instead of original clustering techniques, the graph-cut algorithm is used to classify tetrahedra
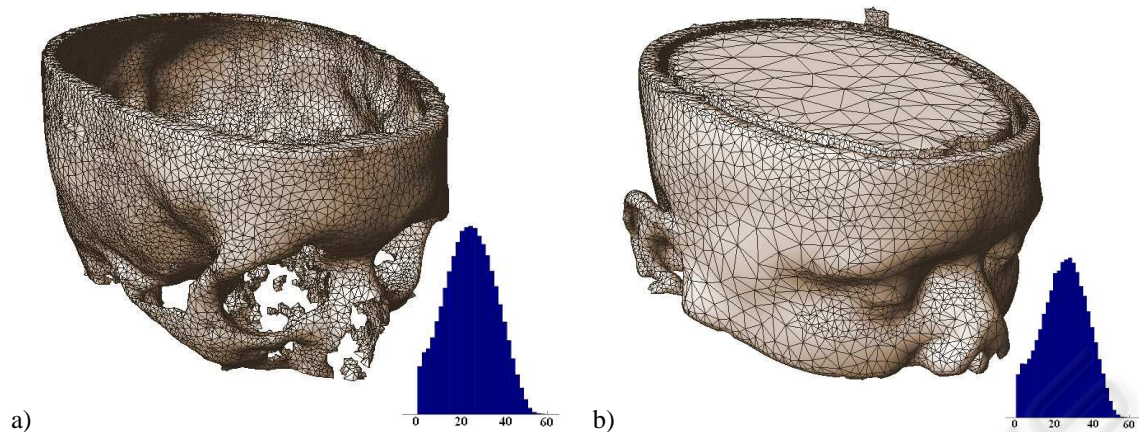
a)   b)

Figure 5: Result of the vector segmentation. Polygonal surfaces of meaningful image regions were extracted directly from the classified tetrahedral mesh: soft tissues (a), hard tissues (b).

into individual regions. Both modifications have improved quality of the output mesh without significant increase of runtime. Besides, there is still space for improvement. It is necessary to deal with slivers, and more sophisticated image features might be incorporated into the mesh classification.

In general, this concept of the volumetric image segmentation has several advantages. Tetrahedral representation of image regions provides continuous approximation of region boundaries (image edges), while the process of raster data vectorization is eliminated. Moreover, a more effective representation of the image structure is obtained. Mesh structure decreases complexity of any classification algorithm that processes a reduced number of tetrahedra instead of voxels.

ACKNOWLEDGEMENTS

REFERENCES

Alliez, P., Cohen-Steiner, D., Yvinec, M., and Desbrun, M. (2005). Variantional tetrahedral meshing. *ACM Trans. Graph.*, 24(3):617–625.

Boykov, Y. and Kolmogorov, V. (2004). An experimental comparison of min-cut/max-flow algorithms for energy minimization in vision. *In IEEE Transactions on PAMI*, 26(9):1124–1137.

Cheng, S. W., Dey, T. K., Edelsbrunner, H., Facello, M. A.,

and Teng, S. H. (1999). Sliver exudation. In *In Proc. 15th ACM Symp. Comput. Geom.*, pages 1–13.

Du, G. and Wang, D. (2003). Tetrahedral mesh generation and optimization based on centroidal voronoi tessellations. *Inter. Journal on Numerical Methods in Engineering*, 56(9):1355–1373.

George, P. L. and Borouchaki, H. (1998). *Delaunay Triangulation and Meshing: Application to Finite Elements*. Editions HERMES, Paris, France.

Gevers, T. (2002). Adaptive image segmentation by combining photometric invariant region and edge information. In *IEEE Trans. on Pattern Analysis and Machine Intelligence*, volume 24.

Lorensen, W. E. and Cline, H. E. (1987). Marching cubes: A high resolution 3d surface construction algorithm. In *SIGGRAPH'87*, volume 21, Anaheim. Computer Graphics.

Owen, S. (1998). A survey of unstructured mesh generation technology. In *Proceedings of the Seventh International Meshing Roundtable*, Dearborn, Michigan. Sandia National Laboratories.

Shewchuk, J. R. (2002). Delaunay refinement algorithms for triangular mesh generation. *Computational Geometry: Theory and Applications*, 22:21–74.

Smith, S. M. and Brady, J. M. (1996). Susan - a new approach to low level image processing. *Inter. Journal of Computer Vision*.

Spanel, M., Krsek, P., Svub, M., Stancl, V., and Siler, O. (2007). Delaunay-based vector segmentation of volumetric medical images. In *In Proc. of CAIP 2007*, pages 261–269. LNCS 4673.